Published in final edited form as:

Pediatr Res. 2023 October ; 94(4): 1355–1364. doi:10.1038/s41390-023-02652-9.

FGF21 Modulates Hippocampal Cold-Shock Proteins and CA2-Subregion Proteins in Neonatal Mice with Hypoxia-Ischemia

Jeremy R. Herrmann[3], **Patrick M. Kochanek**[3], **Vincent A. Vagni**[3], **Keri Janesko-Feldman**[3], **Jason Stezoski**[3], **Kiersten Gorse**[1,2], **Travis C. Jackson**[1,2,*]

[1]University of South Florida, Morsani College of Medicine, USF Health Heart Institute, MDD 0630, 560 Channelside Dr, Tampa, FL 33602

[2]University of South Florida, Morsani College of Medicine, Department of Molecular Pharmacology & Physiology, 12901 Bruce B Downs BLDV, Tampa, FL 33612-4799

[3]Department of Critical Care Medicine, Safar Center for Resuscitation Research, UPMC Children's Hospital of Pittsburgh, Rangos Research Center – 6th floor, Pittsburgh, PA 15224

Abstract

BACKGROUND: Fibroblast growth factor 21 (FGF21) is a neuroprotectant with cognitive enhancing effects but with poorly characterized mechanism(s) of action, particularly in females. Prior studies suggest that FGF21 may regulate cold-shock proteins (CSPs) and CA2-marker proteins in the hippocampus but empirical evidence is lacking.

METHODS: We assessed in normothermic postnatal day (PND) 10 female mice, if hypoxic-ischemic (HI) brain injury (25mins 8% O_2 /92% N_2) altered endogenous levels of FGF21 in serum or in the hippocampus, or its receptor β-Klotho. We also tested if systemic administration of FGF21 (1.5 mg/kg) modulated hippocampal CSPs or CA2 proteins. Finally, we measured if FGF21 therapy altered markers of acute hippocampal injury.

RESULTS: HI increased endogenous serum FGF21 (24h), hippocampal tissue FGF21 (4d), and decreased hippocampal β-Klotho levels (4d). Exogenous FGF21 therapy modulated hippocampal CSP levels, and dynamically altered hippocampal CA2 marker expression (24h and 4d). Finally, FGF21 ameliorated neuronal damage markers at 24h but did not affect GFAP (astrogliosis) or Iba1 (microgliosis) levels at 4d.

CONCLUSIONS: FGF21 therapy modulates CSP and CA2 protein levels in the injured hippocampus. These proteins serve different biological functions, but our findings suggest that FGF21 administration modulates them in a homeostatic manner after HI.

*Corresponding Author: Travis C. Jackson, University of South Florida, Morsani College of Medicine, USF Health Heart Institute, MDD 0630, 560 Channelside Dr, Tampa, FL 33602, Phone: 813-974-2899, Fax: 813-396-0143, tcjackson@usf.edu.

Author Contributions

TCJ conceived the study. TCJ, JRH and PMK contributed to the study design. JRH and TCJ drafted the manuscript. VAV, KG, KJF, and JS contributed to experiments and data acquisition. TCJ, PMK, and JRH contributed to data analysis. PMK, VAV, KG, and KJF edited the draft and contributed to the final submitted version.

Disclosures

Travis C Jackson and Patrick M Kochanek are co-inventors on USPTO patent applications (No. 15/573,006 and 18/166,290) titled: "Method to Improve Neurologic Outcomes in Temperature Managed Patients".

Consent Statement: No consent statement required.

Introduction

Neonatal encephalopathy (NE) is a leading cause of death and disability in newborns[1]. Hypoxia-ischemia (HI) is a major etiology of NE[2–4]. Often the hippocampus is damaged in newborns with perinatal asphyxia (PA) and contributes to cognitive impairment[5,6]. Additional therapies are desperately needed to improve neurologic outcomes in normothermic patients, or to enhance the benefit in newborns that qualify for therapeutic hypothermia (HI)[7,8].

Treatment with fibroblast growth factor 21 (FGF21), a hormone induced by prolonged cold exposure, decreased hippocampal damage and improved long-term cognitive recovery in normothermic postnatal day (PND) 7 rats in the Rice-Vannucci (RV) model of newborn HI[9,10]. We reported that hippocampal-localized FGF21 receptor mechanisms (i.e., β-klotho) are expressed only in newborns, which is distinct from β-klotho receptors in the periphery found throughout life[11–14]. In developing neurons FGF21 is known to regulate a few kinases including AKT, ERK, and GSK-3β, but other proteins may be targeted as well[9,15].

We reviewed the literature for clues on novel targets that could be regulated by FGF21 and that led us to prioritize 2 promising signaling pathways to assess in FGF21 treated neonatal mice. The first was the “cold-shock protein (CSP) pathway” - a group of proteins that can be increased by prolonged hypothermia and that promote hippocampal survival and function by targeting the CA1[16], CA3[17], and DG[18]. Two studies supported a link between FGF21 and CSP induction. One observed that FGF21 augmented the levels of the neuroprotective CSP *RNA-binding motif 3* (RBM3) in immature neurons, and the other inferred that peripheral FGF21 and RBM3 levels are co-regulated in stroke patients[19,20]. FGF21 is also induced by cold, and is thus, poised to regulate CSPs[10]. It has not been tested if FGF21 modulates *cold-induced RNA-binding protein* (CIRBP) or the CSP *reticulon-3* (RTN3). The second pathway we prioritized was the “CA2 marker protein pathway” that includes a group of specialized proteins uniquely abundant in the CA2 hippocampal subregion and which modulate CA2 neuronal survival and function[21]. A single study supported a link between FGF21 and the CA2. Specifically, chronically elevated FGF21 levels in mice uniquely increased metabolic activity in the CA2 subregion of the brain[22]. Coincidently, CA2 neurons are also highly sensitive to damage in the RV model[23]. Thus, modulating CSP and CA2 protein levels may have synergistic benefits on hippocampal health by targeting different subregions including the CA1, CA2, CA3, and the DG.

Here we characterized endogenous levels of serum FGF21, and hippocampal FGF21, β-klotho, and CSPs (RBM3/CIRBP/RTN3) at 1-, 4-, and 8-days post-injury in normothermic female PND10 mice. We used females to build on prior male-only studies in which we initially characterized hippocampal CSP changes in our temperature-controlled RV model. We next tested if exogenous FGF21 therapy (1.5 mg/kg): (1) counteracted the effect of HI to decrease hippocampal CSP levels at 24h- and 4d-post-injury, (2) altered hippocampal CA2 markers including *regulator of G-protein signaling 14* (RGS14), *Purkinje cell protein 4* (PCP4/PEP19), and *N-terminal EF-hand calcium binding protein 2* (NECAB2), and (3) was associated with a decrease in markers of acute tissue injury.

Materials & Methods

Additional details on the reagents and protocols are provided in the Supplementary Methods. An abbreviations table is also provided in the supplementary (Supplementary Table 1).

Animals.

HI studies were approved by the IACUC of the University of Pittsburgh and performed at the Safar Center for Resuscitation Research. Tissues were analyzed at the University of South Florida.

HI Injury Model.

A detailed description of our HI model was reported[23]. Isoflurane anesthetized PND 10 pups (3% induction and 1.5–3% maintenance in a 2:1 mixture of N_2O/O_2) were weighed and core temperature was monitored during surgery (sham or occlusion) via a neonatal rectal probe (Physitemp). Body temperature (T_b) was maintained to ~36°C, which is the normothermic cage-nesting temperature of naïve PND10 pups in our setup[23]. Post-surgical temperature was measured with an infra-red pediatric thermometer (IRT) (Braun Healthcare US). The accuracy of the IRT relative to rectal temperature was previously validated in PND10 mice[23]. The right common carotid artery (CCA) was accessed, ligated, and cut. The incision was closed with 3M Vetbond Tissue Adhesive (Maplewood) and Bupivacaine (0.25%) applied to the wound. Mice advanced in blocks of four[23]. A second technician working in tandem maintained pup temperatures to ~36°C during the post-surgical phase. The four-pup block was then returned to the foster dam for 1h. Pups were placed inside an acrylic hypoxia chamber glove box (Coy; Grass Lake, MI) and subjected to 25 min hypoxia (8% O_2 / 92% N_2). T_b was monitored via IRT during hypoxia and maintained to ~36°C. Shams received surgical procedures without CCA ligation and were placed inside the chamber for 25 min at normoxia (21% O_2 /79% N_2). After hypoxia or normoxia, T_b was managed to ~36°C in room air for 2h:5mins on a benchtop with lamps and heating blankets, and temperature recorded every 15 mins. In neuroprotection studies, pups were randomized to sham/HI and given subcutaneous (SQ) injections of vehicle (0.1% bovine serum albumin in PBS) or 1.5mg/kg mouse-protein recombinant FGF21 (R&D Systems/Biotechne; Minneapolis, MN) 5-min post-HI and returned to dams until weaning or euthanasia. Blinding was not done for cell signaling studies. For the 4d endpoint studies, additional doses were administered SQ in 24h intervals (i.e., 4 doses in total for 4d studies). Cages were supplemented with multiple types of bedding (e.g., Enviro-dri®) to promote high-quality nest construction and decrease thermal stress from standard housing conditions[23].

Neuronal SHSY5Y Cell Culture.

Cell culture studies were approved by the Institutional Biosafety Committee of the University of South Florida. Human neuronal SHSY5Y cells were obtained from ATCC (Manassas, VA), cultured as we reported, and used for experiments at P6[24].

Western Blot.

We used our standard protocol[11]. In brief, brain tissues were homogenized by sonication in inhibitors-supplemented RIPA buffer to generate total protein extracts and analyzed on SDS-PAGE.

ELISA Assay.

Serum was obtained by cardiac puncture at euthanasia. Serum was available from 5/8 PND11 sham pups and 7/8 PND11 HI-injured pups. In older pups, serum samples were available for all sham/HI pups (8/8) at the 4d and 8d post-injury timepoints. The 44 samples in total were then diluted 1:4 or 1:9 and assayed (in duplicate) on a Mouse/Rat FGF21 ELISA Kit (ProteinTech, Cat# KE10042). Concentrations were calculated based on a linear standard curve (in triplicate) and multiplied by a dilution factor of 5 or 10, respectively. Two of 44 samples had values outside the standard curve range (1–1,000 pg/mL). One sample in the 8d HI group had a value below the limit of detection and was recorded as zero for statistics. The other had an extrapolated value of 1,070 pg/mg FGF21. The R-squared of the FGF21 standard curve in each ELISA test was 0.998 and 0.992.

Statistical Analysis.

Western blot densitometry of total protein stain (TPS) and individual targets were measured with UN-SCAN-IT software (Silk Scientific). For each blot, we divided TPS normalized densitometric values by the largest normalized intrablot value to distribute the results on a 0–1 scale to express the data as the “relative difference” for between group comparisons. Data on individual targets from multiple blots were combined and normality assessed using the Kolmogorov-Smirnov test. If passed, a standard parametric factorial ANOVA or 2-Way-ANOVA was used. If failed, a Kruskal-Wallis was applied for factorial ANOVA. For non-parametric multifactorial data, the data were transformed using the Aligned Rank Transformation (ART) tool[25]. The ranked data were then analyzed by standard factorial ANOVA or unpaired t-test for each individual factor (i.e., age, injury, interaction term) to obtain omnibus p-values. For pairwise comparisons, a fourth ranking was done using the recently developed ART-Contrasts (ART-C) algorithm[26], which does not inflate Type I error rates on post-hoc testing. Tukey’s multiple comparison was used for post-hoc significance tests in parametric ANOVAs. Dunn’s multiple comparison was used for post-hoc significance tests with non-parametric Kruskal-Wallis ANOVA. The vehicle-HI group was established as the control for pairwise comparisons in FGF21 therapy studies. Data were significant at $p<0.05$ and graphed using GraphPad Prism.

Results

There was a significant age and injury interaction in serum FGF21, detected on post-hoc as a trend ($p=0.06$) for increased levels at 24h-post-injury (Fig. 1A). There was also a significant age and injury interaction for hippocampal FGF21 tissue levels. On post-hoc, hippocampal FGF21 levels increased at 4d-post-injury, and had an age-dependent increase from PND −14 vs. −18 in shams (Fig. 1B and 1C, and Supplementary Fig. 1). Transmembrane β-klotho is a ~120 kDa protein in mice and we detected a single ~120 kDa band in PND10 mouse brain membrane-enriched extracts (Fig. 1D). Hippocampal β-Klotho levels had an age and

injury interaction, detected on post-hoc as a decrease at 4d-post-injury and an age-dependent increase from PND −11 vs. −14 in shams (Fig. 1E and 1F, and Supplementary Fig. 2).

We previously assessed RBM3, CIRBP, and RTN3 levels in the hippocampus, cortex, and thalamus, in normothermic PND10 male shams vs. HI-injured pups[23]. It was necessary here to use different Lot #s of the RBM3 and RTN3 antibodies. All 3 antibodies identified a dominant band at the correct molecular weight in human neuronal SHSY5Y cells subjected to 48h cooling (Fig. 2A–E and Supplementary Fig. 3). Each CSP displayed different sensitivities to cold induction on 2 clinically relevant depths of hypothermia (i.e., 33°C and 30°C vs. 37°C).

Next, we studied if age and insult affected CSP levels in the normothermic hippocampus, cortex, and thalamus in female pups. Hippocampal RBM3 and RTN3 levels decreased (Fig. 2F, 2G, and 2I, Supplementary Fig. 4, and Supplementary Fig. 5), whereas CIRBP levels increased with age (Fig. 2F and 2H, and Supplementary Fig. 6). Post-hoc analysis detected increased RBM3 and CIRBP levels at 8d-post-injury vs. sham (Fig. 2G and 2H). Cortical RBM3 and RTN3 levels also decreased with age (Supplementary Fig. 7A–B and 7E–F, Supplementary Fig. 8, and Supplementary Fig. 9), whereas CIRBP levels were stable (Supplementary Fig. 7C–D, and Supplementary Fig. 10). Post-hoc analysis showed decreased cortical RBM3 levels at 24h-post-injury and increased RTN3 levels at 8d-post-injury (Supplementary Fig. 7B and 7F). Cortical CIRBP levels increased post-insult but were detected only as a main effect on ANOVA (Supplementary Fig. 7C and 7D). Thalamic, RBM3 and RTN3 levels decreased with age from PND −11 to −18 (Supplementary Fig. 11A–B and 11E–F, Supplementary Fig. 12, and Supplementary Fig. 13), whereas CIRBP levels were stable (Supplementary Fig. 11C–D, and Supplementary Fig. 14). HI did not affect thalamic RBM3 or CIRBP, but did alter RTN3 levels detected as a main effect on ANOVA (Supplementary Fig. 11).

Next, we studied if FGF21 therapy altered hippocampal CSPs at 24h- and 4d- post-injury. Hippocampal RBM3 levels decreased at 24h- and 4d- post-injury in vehicle-treated HI-injured vs. age-matched shams but were unaffected by FGF21 treatment (Fig. 3A–C and 3F, and Supplementary Fig. 15 and 16). Hippocampal CIRBP levels decreased at 24h-post-injury in vehicle-treated HI-injured pups vs. shams and were increased by FGF21 treatment (Fig. 3A and 3D, and Supplementary Fig. 15). CIRBP levels were not affected by HI at 4d-post-injury but were increased by FGF21 treatment (Fig. 3B and 3G, and Supplementary Fig. 16). Hippocampal RTN3 levels increased with HI at 24h-post-injury but were not affected by FGF21 treatment (Fig. 3A and 3E, and Supplementary Fig. 15). HI did not affect 4d-post-injury RTN3 levels but they were increased by FGF21 treatment (Fig. 3B and 3H, and Supplementary Fig. 16).

Next, we assessed CA2 marker proteins. Hippocampal RGS14 levels decreased after HI at 24h-post-injury and were further decreased by FGF21 treatment (Fig. 4A and 4C, and Supplementary Fig. 17). No between-group differences were detected at 4d-post-injury (Fig. 4B and 4F, and Supplementary Fig. 18). Hippocampal PCP4 levels were not affected by HI at 24h-post-injury but were increased by FGF21 treatment (Fig. 4A and 4D, and Supplementary Fig. 17). PCP4 levels were also not affected by HI at the 4d-post-injury

time point, but conversely, were decreased by FGF21 treatment (Fig. 4B and 4G, and Supplementary Fig. 18). Hippocampal NECAB2 levels were decreased by HI at 24h-post-injury but were not affected by FGF21 treatment (Fig. 4A and 4E, and Supplementary Fig. 17). Conversely, NECAB2 levels were increased at 4d-post-injury but again were not affected by FGF21 treatment (Fig. 4B and 4H, and Supplementary Fig. 18).

Finally, we measured acute cell death and gliosis markers in the hippocampus. Also, to replicate previous studies on these targets in male pups after HI, we first assessed the age course samples harvested from female mice at 1d-, 4d-, and 8d- postinjury. HI increased α-II-spectrin breakdown products, detected as a main effect on ANOVA (SBDPs; Fig. 5A–B, and Supplementary Fig. 19A, 19C, and 19D). Total poly(ADP-ribose) polymerase (tPARP) decreased after HI at 24h- and 4d-post-injury (Fig. 5A and 5C, and Supplementary Fig. 19B, 19E, and 19F). Glial fibrillary acidic protein (GFAP) levels were increased at 4d- and 8d-post-injury (Fig. 5A and 5D and Supplementary Fig. 19A, 19C, and 19D). Ionized Ca^{+2}-binding adapter protein 1 (Iba1) levels were increased at 8d-post-injury (Fig. 5A and 5E, and Supplementary Fig. 19B, 19E, and 19F).

Regarding the effect of drug therapy on these targets, SBDP levels were increased by HI at 24h-post-injury but were not significantly affected by FGF21 treatment (Fig. 6A and 6C, and Supplementary Fig. 20). However, 1/8 hippocampi in the FGF21-treated HI group vs. 5/8 in the vehicle-treated HI group had SBDP signals. tPARP levels were decreased by HI and were increased by FGF21 treatment (Fig. 6A and 6D, and Supplementary Fig. 20). It was reported that 1.5mg/kg FGF21 increased posphorylated AKT (pAKT473) at 24h-post-injury in the rat hippocampus in the RV model[9]. Here, in the mice RV model, 1.5mg/kg FGF21 did not increase hippocampal pAKT473 at 24h post-injury (Supplementary Fig. 20 and Supplementary Fig. 21). Finally, GFAP and Iba1 levels were not affected by FGF21 treatment (Fig. 6A, 6E, 6F, and Supplementary Fig. 20).

Discussion

The objectives of this study were (1) to test if HI in the RV model affected endogenous FGF21 or hippocampal β-klotho tissue levels at 1-, 4-, and 8d-post-injury, (2) to replicate time course investigations previously reported in males on CSPs after HI in female pups in the hippocampus, cortex, and thalamus[23], and (3) to test if FGF21 therapy (1.5 mg/kg, SQ) modulated CSPs, CA2-markers, or classic tissue injury markers.

Endogenous FGF21 has not been studied in HI-injured neonates[9]. Serum FGF21 increased 24h after HI in mouse pups, consistent with studies in children after cardiac arrest[27]. The source of serum FGF21 was not investigated. We speculate that it is liver-derived because hepatic secretion is the primary source in neonates, and because systemic hypoxia triggers FGF21 liver secretion in adults[28,29]. We also observed an age-related decline in serum FGF21 levels, whereas hippocampal tissue levels increased with age at the same time points including in shams. That novel finding merits additional study and may relate to novel sources of endogenous FGF21 in the brain that target the hippocampus[30]. We also speculate that the discord between elevated serum vs. stable hippocampal FGF21 levels at 24h post-injury may be due to compromised blood flow to injured brain tissue, and more studies

are needed to determine if targeting pharmacological levels using high dose bolus therapy are required for neuroprotection. Nevertheless, endogenous FGF21 may be beneficial in neonates via targeting both central and peripheral mechanisms. Consistent with that notion, adult FGF21 KO mice with stroke had worse neurological outcomes, presumably caused by loss of peripheral FGF21 receptor activation[31]. Germane to the effect of HI on central FGF21 receptors in neonates, we also observed decreased hippocampal β-klotho levels at 4d-post-injury.

RBM3 and RTN3 levels decreased with age from PND 11–18 in the female hippocampus, cortex, and thalamus (in shams and injured mice), similar to our prior findings in males in this model[23]. Curiously, CIRBP levels increased with age or were stable in the female hippocampus, cortex, and thalamus. Supplementary Tables 2 and 3 highlight the similarities and differences in the abundance of CSPs at the same time points in males vs. females (i.e., based on comparison to our 2022 study[23]). In females RBM3 levels also decreased at 24h-post-injury in the hippocampus and cortex and were robustly increased at 8d-post-injury. RBM3 inhibits apoptosis and hippocampal lesions are exacerbated in RBM3 KO mice after ischemia[18]. The acute loss of RBM3 is consistent with known sex-dependent differences on the mechanisms mediating cell death in females with neonatal HI[32].

FGF21 therapy did not increase hippocampal RBM3 levels at 24h- or 4d-post-injury, but we detected a trend for an effect. More strikingly, FGF21 therapy increased hippocampal CIRBP protein levels at 24h- and 4d-post-injury. Treatment also increased hippocampal RTN3 levels at 4d-post-injury. Notably, CIRBP levels were not affected 24h-post-HI in the time course studies but decreased in the FGF21 treatment studies. That could be due to litter effects, differences in insult severity, or stress effects from manipulations associated with injections.

Our findings on the effect of FGF21 on CSPs raise additional questions. RBM3 mediates hibernation-induced neuroprotection[16,18]. It also protects the fetal brain *in utero* from hypothermia-mediated structural derangements, which explains its temporary abundance at birth in the normothermic brain[33]. Similarly, CIRBP KO mice have increased hippocampal and BBB damage in a hypothermia model of cardiopulmonary bypass[34]. Finally, RTN3 promotes axonal growth and contributes to cooling-induced neuroprotection[35,36]. CSPs are also linked with neuroprotection of the hippocampal CA1[16,37], CA3[17,38], and DG[18,38] subregions.

The CA2 subregion is also prone to damage in the HI model and may be a clinical target in NE[23]. Thus, we also explored proteins that modulate CA2 survival and function. FGF21 concomitantly decreased hippocampal RGS14 levels and increased PCP4 levels at 24h-post-injury. At 4d-post-injury, FGF21 did not affect RGS14 levels but decreased PCP4 levels. It is not clear if the delayed decrease may have been produced by sustained activation of this novel mechanism by repeat dosing. Finally, HI insult, but not FGF21, therapy affected NECAB2 levels.

Our findings on the effect of FGF21 on CA2 proteins also raise more questions. We speculate that a therapeutic decrease in RGS14 levels at 24h post-HI might be

beneficial. Overexpression of RGS14 impaired synaptic plasticity in the CA2 and worsened performance on learning and memory tests[39]. In contrast, a therapeutic increase in PCP4 levels may be beneficial. Indeed, PCP4 overexpression was neuroprotective in a model of glutamate excitotoxicity[40]. The possibility that FGF21 has homeostatic effects on multiple beneficial pathways across multiple hippocampal subregions is an exciting new avenue of research for future exploration.

FGF21 did not affect NECAB2 but it was consistently decreased at 24h post-injury and increased at 4d-post-injury. That surprised us given the variability of insult produced in the RV model (e.g., supported by variability in the levels of SBDPs, Iba1, and GFAP across animals). Thus, NECAB2 may be a highly reproducible novel marker of brain damage in neonatal HI but the consequences of its dysregulation need to be determined.

To infer a potential effect of FGF21 on hippocampal health we measured several classic markers of brain damage. Increased SBDP levels (145–150 kDa) suggests necrosis[41]. FGF21 treatment resulted in fewer SBDP-positive hippocampi vs. vehicle controls (1/8 vs. 5/8). The mean difference was not statistically significant and we were underpowered to test this outcome based on the large standard deviation for this target. Additional studies with larger sample sizes are needed and in males to appropriately test that hypothesis. Loss of tPARP is a signature of apoptotic neuronal death[42]. FGF21 therapy prevented tPARP degradation in HI-injured mice. Numerous proteases cleave tPARP and the enzymes responsible in our model need to be elucidated[42]. Finally, FGF21 treatment did not decrease astrocytic GFAP or microglial Iba-1 levels 4d post-injury. The latter result does not necessarily suggest a therapeutic limitation given that in adults FGF21-mediated astrocytic activation contributes to neuroprotection[43,44]. Also, the use of females here may have limited an assessment of the effect of FGF21 on microglia given that neuroinflammation in newborns with HI is sex-dependent and microgliosis is more robust in males[45,46].

There were study limitations. First, the group size limited our ability to detect small effects of FGF21 therapy which may prove important (e.g., modulation of RBM3) and blinding was not done. Second, only females were used, thus, it remains unclear if FGF21 modulates CSPs and CA2 proteins in males[47]. Third, we did not study FGF21 therapy in uninjured pups. Fourth, FGF21 may increase “CA2 markers” in other brain regions[48] and histology is needed to shed light on their location(s), cell type(s), and distribution. However, within the PND11-PND14 mouse hippocampus, all three CA2 proteins are highly selective for CA2 neurons[21]. Finally, we did not assess histological or neurobehavioral outcomes.

In summary, it was recently reported that FGF21 therapy improved hippocampal survival and function in the RV model[9] and its neuroprotective effects are well established in other models of brain injury as well[31,49,50]. The molecular underpinnings are unknown. Here we identified several novel targets - members of the CSP and CA2 protein pathways that regulate both hippocampal survival and function[16,36,37,39,40,51–55]. They represent promising new candidates for future study in ongoing efforts to define the mechanism(s) mediating FGF21-induced neuroprotection.

Supplementary Material

Refer to Web version on PubMed Central for supplementary material.

Financial Support

This work was supported by NIH/NINDS grant R01NS105721 to TCJ, by the University of South Florida Morsani College of Medicine start-up funds to TCJ, by a Lloyd Reback Family Gift, Laerdal Foundation for Acute Medicine grant, Zoll Foundation grant, and T32 (2T32HD040686) to JRH, and by the Ake N. Grenvik Chair in Critical Care Medicine to PMK.

Data Availability

All data generated or analyzed during this study are included in this published article and its supplementary files.

References

1. Lawn JE et al. Every Newborn: Progress, Priorities, and Potential Beyond Survival. Lancet 384, 189–205 (2014). [PubMed: 24853593]
2. Lee AC et al. Intrapartum-Related Neonatal Encephalopathy Incidence and Impairment at Regional and Global Levels for 2010 with Trends from 1990. Pediatr Res 74 Suppl 1, 50–72 (2013). [PubMed: 24366463]
3. Acun C et al. Trends of Neonatal Hypoxic-Ischemic Encephalopathy Prevalence and Associated Risk Factors in the United States, 2010 to 2018. Am J Obstet Gynecol (2022).
4. Sandoval Karamian AG et al. Neonatal Encephalopathy: Etiologies Other Than Hypoxic-Ischemic Encephalopathy. Semin Fetal Neonatal Med 26, 101272 (2021). [PubMed: 34417137]
5. Schiering IA et al. Correlation between Clinical and Histologic Findings in the Human Neonatal Hippocampus after Perinatal Asphyxia. J Neuropathol Exp Neurol 73, 324–334 (2014). [PubMed: 24607964]
6. Maneru C et al. Residual Hippocampal Atrophy in Asphyxiated Term Neonates. J Neuroimaging 13, 68–74 (2003). [PubMed: 12593134]
7. Thayyil S et al. Hypothermia for Moderate or Severe Neonatal Encephalopathy in Low-Income and Middle-Income Countries (Helix): A Randomised Controlled Trial in India, Sri Lanka, and Bangladesh. Lancet Glob Health 9, e1273–e1285 (2021). [PubMed: 34358491]
8. Tagin MA, Woolcott CG, Vincer MJ, Whyte RK & Stinson DA Hypothermia for Neonatal Hypoxic Ischemic Encephalopathy: An Updated Systematic Review and Meta-Analysis. Arch Pediatr Adolesc Med 166, 558–566 (2012). [PubMed: 22312166]
9. Ye L et al. Fgf21 Promotes Functional Recovery after Hypoxic-Ischemic Brain Injury in Neonatal Rats by Activating the Pi3k/Akt Signaling Pathway Via Fgfr1/Beta-Klotho. Exp Neurol 317, 34–50 (2019). [PubMed: 30802446]
10. Lee P et al. Mild Cold Exposure Modulates Fibroblast Growth Factor 21 (Fgf21) Diurnal Rhythm in Humans: Relationship between Fgf21 Levels, Lipolysis, and Cold-Induced Thermogenesis. J Clin Endocrinol Metab 98, E98–102 (2013). [PubMed: 23150685]
11. Jackson TC, Kotermanski SE & Kochanek PM Infants Uniquely Express High Levels of Rbm3 and Other Cold-Adaptive Neuroprotectant Proteins in the Human Brain. Dev Neurosci 40, 325–336 (2018). [PubMed: 30399610]
12. Jackson TC, Janesko-Feldman K, Carlson SW, Kotermanski SE & Kochanek PM Robust Rbm3 and Beta-Klotho Expression in Developing Neurons in the Human Brain. J Cereb Blood Flow Metab, 271678X19878889 (2019).
13. Bookout AL et al. Fgf21 Regulates Metabolism and Circadian Behavior by Acting on the Nervous System. Nat Med 19, 1147–1152 (2013). [PubMed: 23933984]

14. Talukdar S et al. Fgf21 Regulates Sweet and Alcohol Preference. Cell Metab 23, 344–349 (2016). [PubMed: 26724861]
15. Leng Y et al. Fgf-21, a Novel Metabolic Regulator, Has a Robust Neuroprotective Role and Is Markedly Elevated in Neurons by Mood Stabilizers. Mol Psychiatry 20, 215–223 (2015). [PubMed: 24468826]
16. Peretti D et al. Rbm3 Mediates Structural Plasticity and Protective Effects of Cooling in Neurodegeneration. Nature 518, 236–239 (2015). [PubMed: 25607368]
17. Liu B et al. The Overexpression of Rbm3 Alleviates Tbi-Induced Behaviour Impairment and Ad-Like Tauopathy in Mice. J Cell Mol Med 24, 9176–9188 (2020). [PubMed: 32648620]
18. Zhu X et al. Rbm3 Promotes Neurogenesis in a Niche-Dependent Manner Via Imp2-Igf2 Signaling Pathway after Hypoxic-Ischemic Brain Injury. Nat Commun 10, 3983 (2019). [PubMed: 31484925]
19. Jackson TC et al. Cold Stress Protein Rbm3 Responds to Temperature Change in an Ultra-Sensitive Manner in Young Neurons. Neuroscience 305, 268–278 (2015). [PubMed: 26265550]
20. Avila-Gomez P et al. Associations between Rna-Binding Motif Protein 3, Fibroblast Growth Factor 21, and Clinical Outcome in Patients with Stroke. J Clin Med 11 (2022).
21. Laham BJ, Diethorn EJ & Gould E Newborn Mice Form Lasting Ca2-Dependent Memories of Their Mothers. Cell Rep 34, 108668 (2021). [PubMed: 33503421]
22. Forsstrom S et al. Fibroblast Growth Factor 21 Drives Dynamics of Local and Systemic Stress Responses in Mitochondrial Myopathy with Mtdna Deletions. Cell Metab 30, 1040–1054 e1047 (2019). [PubMed: 31523008]
23. Jackson TC et al. Hypoxia-Ischemia-Mediated Effects on Neurodevelopmentally Regulated Cold-Shock Proteins in Neonatal Mice under Strict Temperature Control. Pediatr Res (2022).
24. Jackson TC et al. The Nuclear Splicing Factor Rna Binding Motif 5 Promotes Caspase Activation in Human Neuronal Cells, and Increases after Traumatic Brain Injury in Mice. J Cereb Blood Flow Metab 35, 655–666 (2015). [PubMed: 25586139]
25. Wobbrock JO, Findlater L, Gergle D & Higgins JJ in Proceedings of the SIGCHI Conference on Human Factors in Computing Systems 143–146 (Association for Computing Machinery, 2011).
26. Elkin LA, Kay M, Higgins JJ & Wobbrock JO in The 34th Annual ACM Symposium on User Interface Software and Technology 754–768 (Association for Computing Machinery, 2021).
27. Herrmann JR et al. Serum Levels of the Cold Stress Hormones Fgf21 and Gdf-15 after Cardiac Arrest in Infants and Children Enrolled in Single Center Therapeutic Hypothermia Clinical Trials. Resuscitation 172, 173–180 (2022). [PubMed: 34822938]
28. Hondares E et al. Hepatic Fgf21 Expression Is Induced at Birth Via Pparalpha in Response to Milk Intake and Contributes to Thermogenic Activation of Neonatal Brown Fat. Cell Metab 11, 206–212 (2010). [PubMed: 20197053]
29. Wu G et al. Hypoxia-Induced Adipose Lipolysis Requires Fibroblast Growth Factor 21. Front Pharmacol 11, 1279 (2020). [PubMed: 32922298]
30. Zhou B et al. Central Fgf21 Production Regulates Memory but Not Peripheral Metabolism. Cell Rep 40, 111239 (2022). [PubMed: 36001982]
31. Mamtilahun M et al. Plasma from Healthy Donors Protects Blood-Brain Barrier Integrity Via Fgf21 and Improves the Recovery in a Mouse Model of Cerebral Ischaemia. Stroke Vasc Neurol 6, 561–571 (2021). [PubMed: 33785536]
32. Weis SN et al. Autophagy in the Brain of Neonates Following Hypoxia-Ischemia Shows Sex- and Region-Specific Effects. Neuroscience 256, 201–209 (2014). [PubMed: 24184979]
33. Xia W, Su L & Jiao J Cold-Induced Protein Rbm3 Orchestrates Neurogenesis Via Modulating Yap Mrna Stability in Cold Stress. J Cell Biol 217, 3464–3479 (2018). [PubMed: 30037926]
34. Liu M et al. Cold-Inducible Rna-Binding Protein as a Novel Target to Alleviate Blood-Brain Barrier Damage Induced by Cardiopulmonary Bypass. J Thorac Cardiovasc Surg 157, 986–996 e985 (2019). [PubMed: 30396738]
35. Wojnacki J et al. Role of Vamp7-Dependent Secretion of Reticulon 3 in Neurite Growth. Cell Rep 33, 108536 (2020). [PubMed: 33357422]

36. Bastide A et al. Rtn3 Is a Novel Cold-Induced Protein and Mediates Neuroprotective Effects of Rbm3. Curr Biol 27, 638–650 (2017). [PubMed: 28238655]
37. Zhou Y et al. Cirbp-Psd95 Axis Protects against Hypobaric Hypoxia-Induced Aberrant Morphology of Hippocampal Dendritic Spines and Cognitive Deficits. Mol Brain 14, 129 (2021). [PubMed: 34419133]
38. Shi Q et al. Reduced Amyloid Deposition in Mice Overexpressing Rtn3 Is Adversely Affected by Preformed Dystrophic Neurites. J Neurosci 29, 9163–9173 (2009). [PubMed: 19625507]
39. Lee SE et al. Rgs14 Is a Natural Suppressor of Both Synaptic Plasticity in Ca2 Neurons and Hippocampal-Based Learning and Memory. Proc Natl Acad Sci U S A 107, 16994–16998 (2010). [PubMed: 20837545]
40. Kanazawa Y et al. Degradation of Pep-19, a Calmodulin-Binding Protein, by Calpain Is Implicated in Neuronal Cell Death Induced by Intracellular Ca2+ Overload. Neuroscience 154, 473–481 (2008). [PubMed: 18502590]
41. Wang KKW Calpain and Caspase: Can You Tell the Difference? Trends in Neurosciences 23, 20–26 (2000). [PubMed: 10631785]
42. Chaitanya GV, Steven AJ & Babu PP Parp-1 Cleavage Fragments: Signatures of Cell-Death Proteases in Neurodegeneration. Cell Commun Signal 8, 31 (2010). [PubMed: 21176168]
43. Sun Y et al. Modulation of the Astrocyte-Neuron Lactate Shuttle System Contributes to Neuroprotective Action of Fibroblast Growth Factor 21. Theranostics 10, 8430–8445 (2020). [PubMed: 32724479]
44. Li Y et al. Maternal High-Fat Diet Alters the Characteristics of Astrocytes and Worsens the Outcome of Stroke in Rat Offspring, Which Improves after Fgf21 Administration. Front Cell Dev Biol 9, 731698 (2021). [PubMed: 35096806]
45. Villapol S et al. Early Sex Differences in the Immune-Inflammatory Responses to Neonatal Ischemic Stroke. Int J Mol Sci 20 (2019).
46. Mirza MA, Ritzel R, Xu Y, McCullough LD & Liu F Sexually Dimorphic Outcomes and Inflammatory Responses in Hypoxic-Ischemic Encephalopathy. J Neuroinflammation 12, 32 (2015). [PubMed: 25889641]
47. Zhu C et al. Different Apoptotic Mechanisms Are Activated in Male and Female Brains after Neonatal Hypoxia-Ischaemia. J Neurochem 96, 1016–1027 (2006). [PubMed: 16412092]
48. Ziai MR, Sangameswaran L, Hempstead JL, Danho W & Morgan JI An Immunochemical Analysis of the Distribution of a Brain-Specific Polypeptide, Pep-19. J Neurochem 51, 1771–1776 (1988). [PubMed: 3183658]
49. Wang D et al. Fgf21 Alleviates Neuroinflammation Following Ischemic Stroke by Modulating the Temporal and Spatial Dynamics of Microglia/Macrophages. J Neuroinflammation 17, 257 (2020). [PubMed: 32867781]
50. Chen J et al. Fgf21 Protects the Blood-Brain Barrier by Upregulating Ppargamma Via Fgfr1/Beta-Klotho after Traumatic Brain Injury. J Neurotrauma 35, 2091–2103 (2018). [PubMed: 29648978]
51. Sertel SM, von Elling-Tammen MS & Rizzoli SO The Mrna-Binding Protein Rbm3 Regulates Activity Patterns and Local Synaptic Translation in Cultured Hippocampal Neurons. J Neurosci 41, 1157–1173 (2021). [PubMed: 33310754]
52. Alhajlah S, Thompson AM & Ahmed Z Overexpression of Reticulon 3 Enhances Cns Axon Regeneration and Functional Recovery after Traumatic Injury. Cells 10 (2021).
53. Wei P, Blundon JA, Rong Y, Zakharenko SS & Morgan JI Impaired Locomotor Learning and Altered Cerebellar Synaptic Plasticity in Pep-19/Pcp4-Null Mice. Mol Cell Biol 31, 2838–2844 (2011). [PubMed: 21576365]
54. Canela L et al. The Association of Metabotropic Glutamate Receptor Type 5 with the Neuronal Ca2+-Binding Protein 2 Modulates Receptor Function. J Neurochem 111, 555–567 (2009). [PubMed: 19694902]
55. Purgert CA et al. Intracellular Mglur5 Can Mediate Synaptic Plasticity in the Hippocampus. J Neurosci 34, 4589–4598 (2014). [PubMed: 24672004]

Impact

- Hypoxic-Ischemic (HI) injury in female post-natal day (PND) 10 mice decreases hippocampal RNA binding motif 3 (RBM3) levels in the normothermic newborn brain.
- HI injury in normothermic newborn female mice alters serum and hippocampal fibroblast growth factor 21 (FGF21) levels 24h post-injury.
- HI injury in normothermic newborn female mice alters hippocampal levels of N-terminal EF-hand calcium binding protein 2 (NECAB2) in a time-dependent manner.
- Exogenous FGF21 therapy ameliorates the HI-mediated loss of hippocampal cold-induced RNA-binding protein (CIRBP).
- Exogenous FGF21 therapy modulates hippocampal levels of CA2-marker proteins after HI.

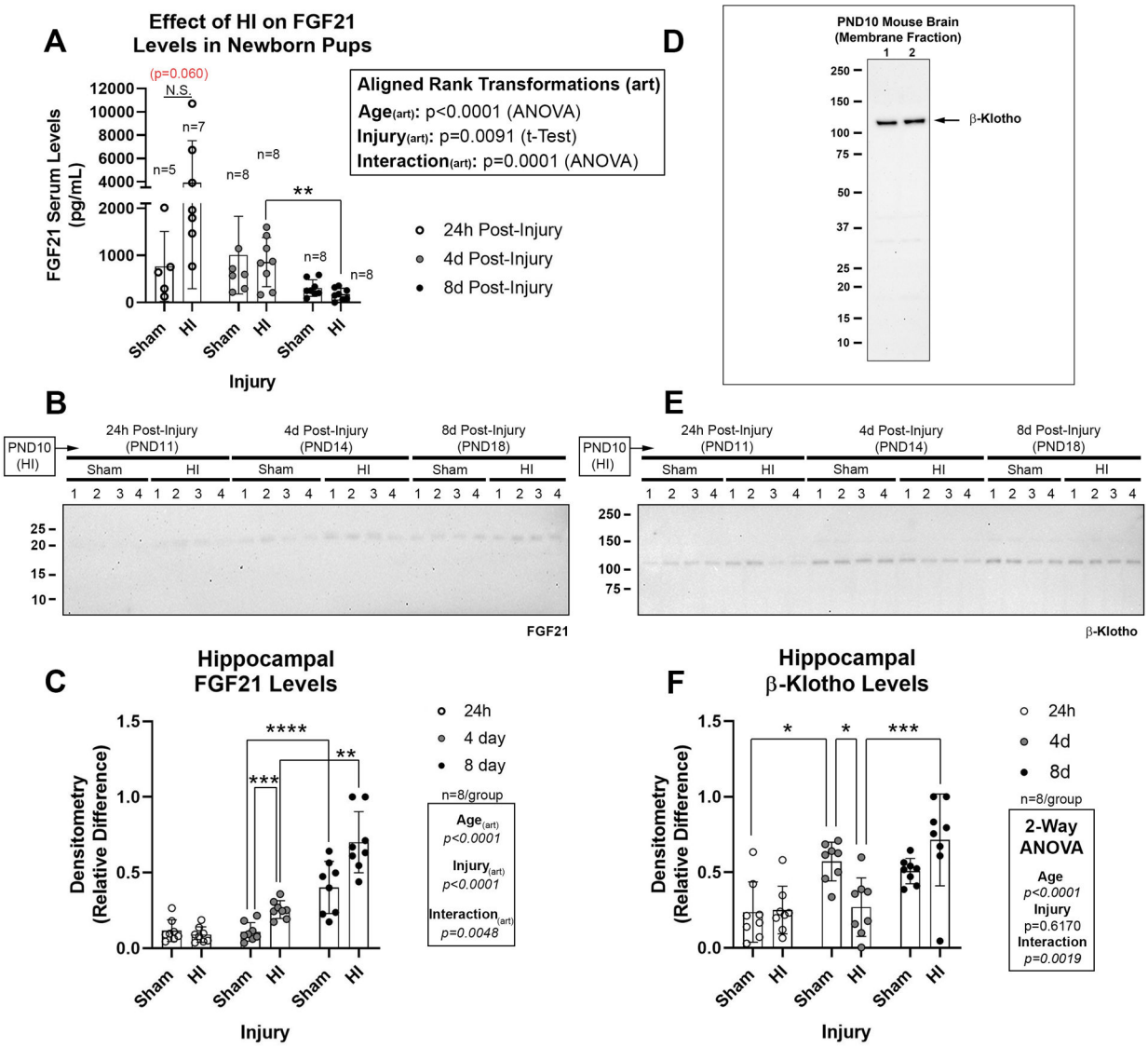

Fig. 1: The Effect of HI on Endogenous FGF21 and Hippocampal β-Klotho Levels.

(A) Serum FGF21 levels in pups at 24h- (n=5/group sham and n=7/group HI), 4d- (n=8/group sham and n=8/group HI), and 8d-post-injury (n=8/group sham and n=8/group HI). **(B)** Representative Western blot (n=4/group) of hippocampal FGF21 in shams vs. HI-injured pups 24h-, 4d-, and 8d-post-injury. **(C)** Densitometry of FGF21 (n=8/group). **(D)** Specificity of β-klotho antibody to detect a ~120 kDa band in membrane-enriched protein fractions from neonatal brain. **(E)** Representative Western blot (n=4/group) of hippocampal β-klotho in shams vs. HI-injured pups 24h-, 4d-, and 8d-post-injury. **(F)** Densitometry of β-klotho (n=8/group). Images of total protein stains used to normalize protein loading are available in the supplementary. Data were significant at $p < 0.05$. Asterisks in graphs indicate post hoc significance. (*) $p<0.05$, (**) $p<0.01$, (***) $p<0.001$, (****) $p<0.0001$, (N.S.) = non-significant. Red highlighted p-values correspond to a N.S. trend on post-hoc.

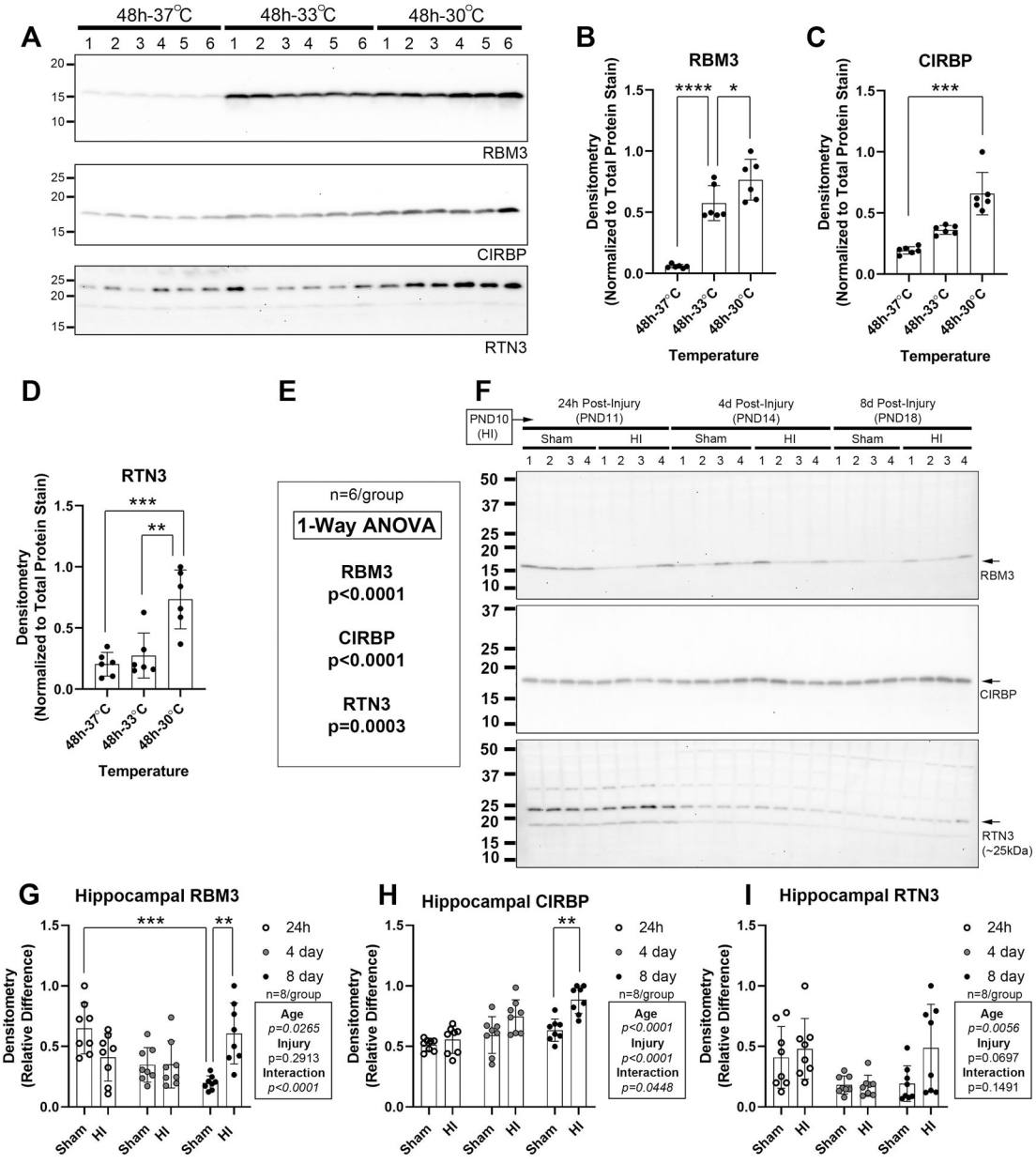

Fig. 2: Validation of CSP detecting Antibodies and the Effect of HI on Neurodevelopmental Expression of Hippocampal CSP Proteins.

Hypothermia experiments in human neuronal SHSY5Y cells were done to validate antibody reagent fidelity to detect CSPs. **(A)** Western blots (n=6/group) show RNA-binding motif 3 (RBM3), cold-inducible RNA-binding protein (CIRBP), and reticulon 3 (RTN3) levels after 48h at 37°C, 33°C, or 30°C. **(B-E)** Densitometry of CSPs (n=6/group). **(F)** Representative Western blot (n=4/group) of hippocampal RBM3, CIRBP, and RTN3 levels in shams vs. HI-injured pups 24h-, 4d-, and 8d-post-injury. **(G, H, & I)** Densitometry of RBM3, CIRBP, and RTN3 levels (n=8/group). Data were significant at $p < 0.05$. Asterisks in graphs indicate post hoc significance. (*) $p<0.05$, (**) $p<0.01$, (***) $p<0.001$, (****) $p<0.0001$.

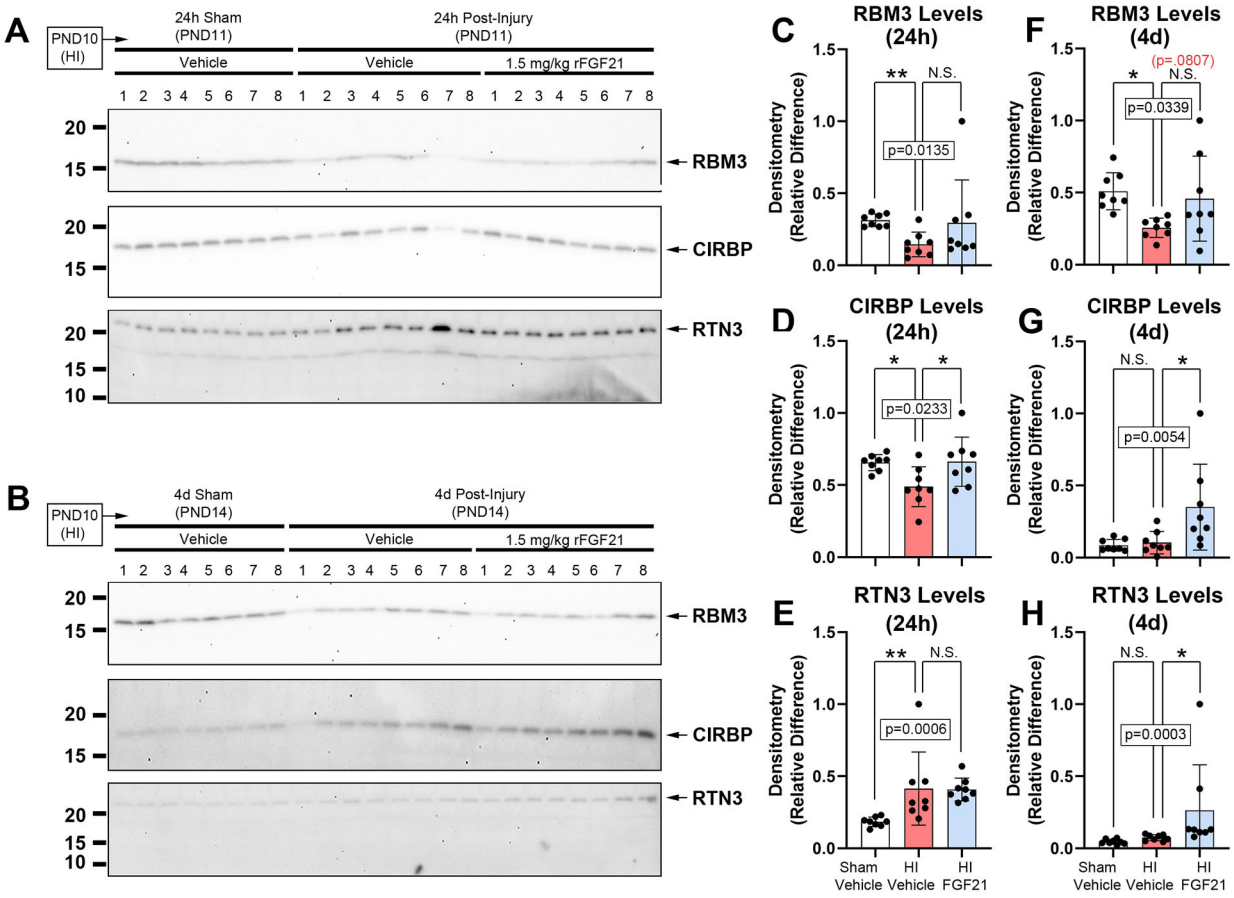

Fig 3. The Effect of FGF21 Administration in HI-Injured Pups on Hippocampal CSPs.

Pups were administered vehicle or 1.5mg/kg FGF21 subcutaneously every 24h (maximum 4 injections) starting 5min-post-injury. **(A** and **B)** Western blot (n=8/group) of hippocampal RBM3, CIRBP, and RTN3 levels in sham-vehicle vs. HI-vehicle vs. FGF21-treated pups at 24h- and 4d post-injury, respectively. **(C, D, E** and **F, G, H)** Densitometry of RBM3, CIRBP, and RTN3 levels (n=8/group) at 24h- and 4d post-injury, respectively. Data were significant at $p < 0.05$. Asterisks in graphs indicate post hoc significance. RNA-binding motif 3 (RBM3), cold inducible RNA-binding protein (CIRBP), reticulon 3 (RTN3). (*) $p<0.05$, (**) $p<0.01$, (N.S.) = non-significant. Red highlighted p-value corresponds to a N.S. trend on post-hoc.

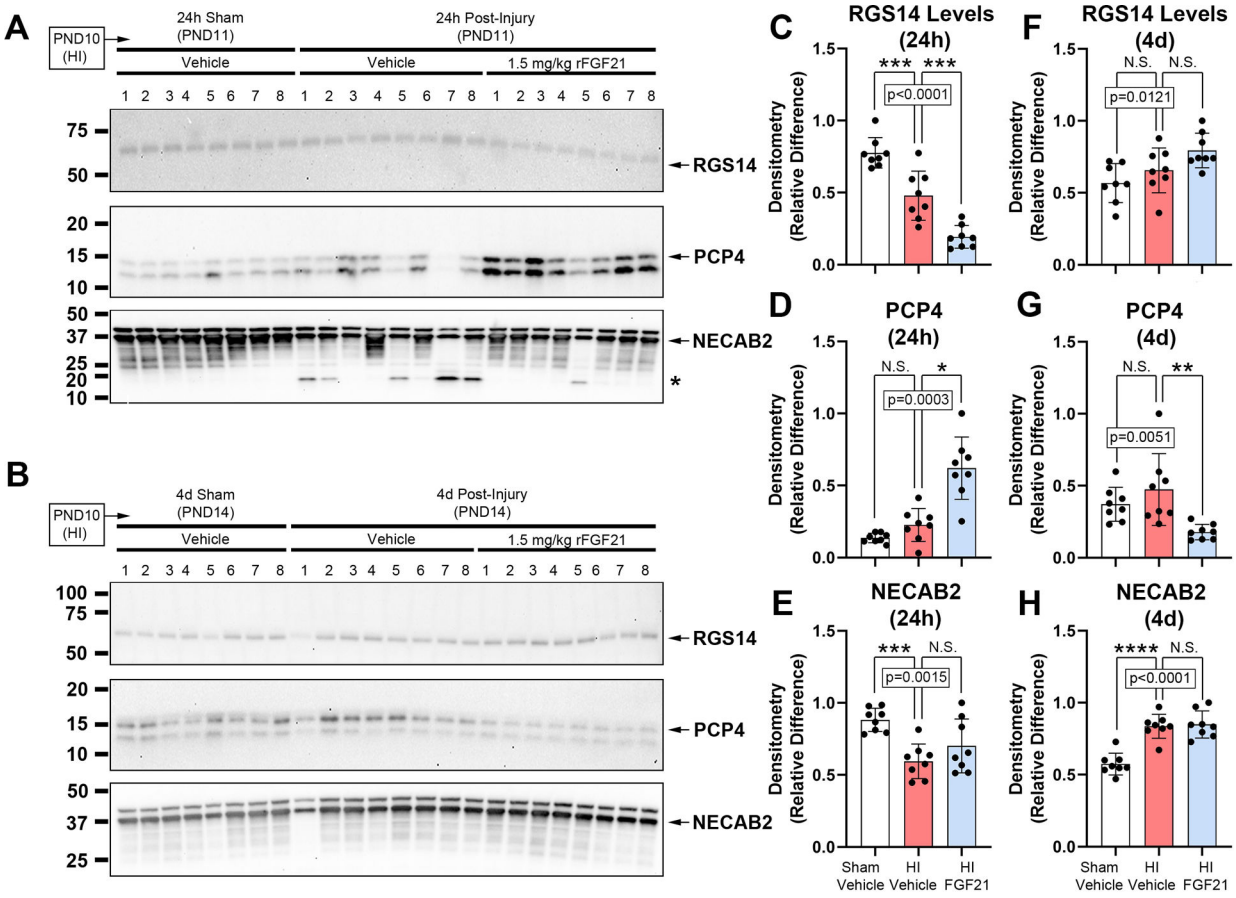

Fig 4. The Effect of FGF21 Administration in HI-Injured Pups on Hippocampal CA2 Marker Proteins.

Pups were administered vehicle or 1.5mg/kg FGF21 subcutaneously every 24h (maximum 4 injections) starting 5-min post-injury. **(A** and **B)** Western blot (n=8/group) of hippocampal RGS14, PCP4, and NECAB2 levels in sham-vehicle vs. HI-vehicle vs. FGF21-treated pups at 24h- and 4d post-injury, respectively. The asterisk on the NECAB2 blot denotes a potential uncharacterized cleavage product. **(C, D, E** and **F, G, H)** Densitometry of RGS14, PCP4, and NECAB2 levels (n=8/group) at 24h- and 4d post-injury, respectively. Data were significant at p <0.05. Asterisks in graphs indicate post hoc significance. (*) p<0.05, (**) p<0.01, (***) p<0.001, (****) p<0.0001, (N.S.) = non-significant. Regulator of G-protein signaling 14 (RGS14), purkinje cell protein 4 (PCP4), N-terminal EF-hand calcium binding protein 2 (NECAB2).

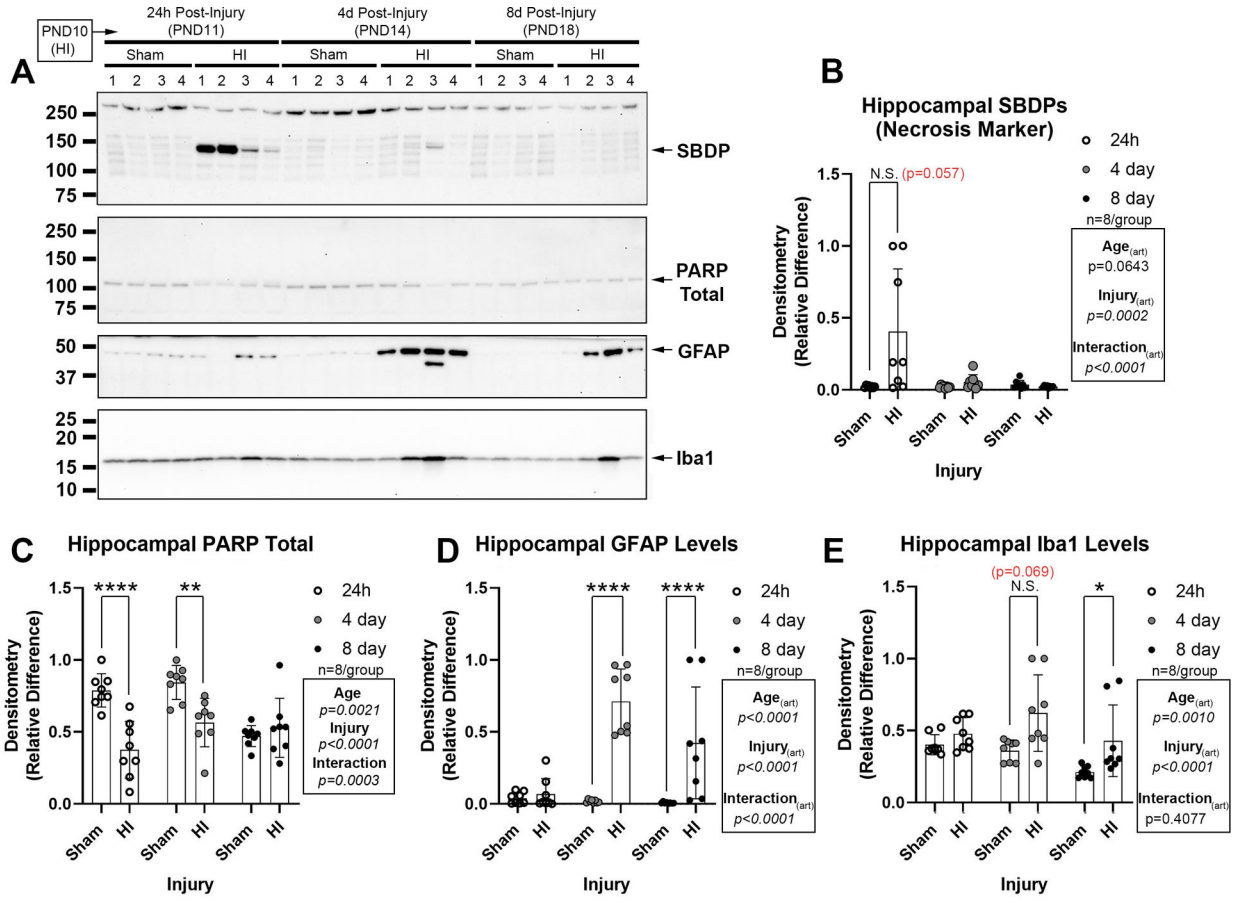

Fig. 5: Acute Brain Injury Markers in Normothermic PND10 Female Mice Subjected to HI.

(A) Representative western blot of brain injury biomarkers. **(B)** The necrosis marker α-II-spectrin breakdown product (SBDP) is increased in the ipsilateral hippocampus at 24h-post-injury. **(C)** Total levels of poly(ADP-ribose)polymerase (PARP) are decreased at 24h- and 4d-post-injury (decreased levels suggest increased cell death). **(D)** The astrogliosis marker glial fibrillary acidic protein (GFAP) is increased at 4d- and 8d-post-injury. **(E)** The microgliosis marker ionized Ca+2-binding adapter protein 1 (Iba1) is increased at 4d post-injury. Western blots are representative images (n=4/group). Graphs of densitometry comprise n=8/group. Data were significant at $p < 0.05$. Asterisks in graphs indicate post hoc significance. (*) $p<0.05$, (**) $p<0.01$, (****) $p<0.0001$, (N.S.) = non-significant. Red highlighted p-value correspond to a N.S. trend on post-hoc.

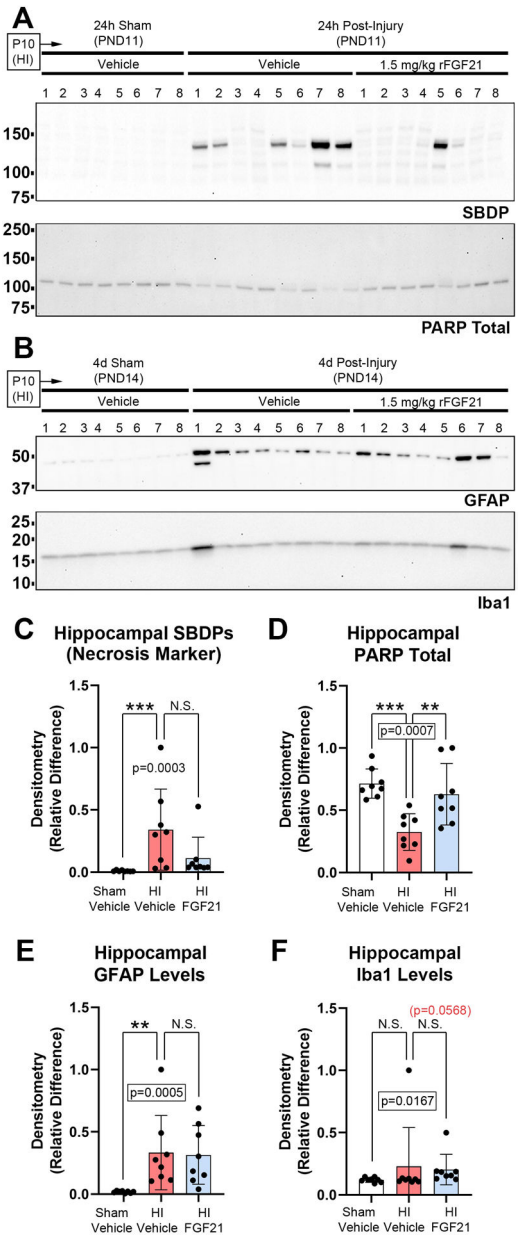

Fig 6. The Effect of FGF21 Administration on Acute Brain Injury Markers.

Pups were administered vehicle or 1.5mg/kg FGF21 subcutaneously every 24h (maximum 4 injections) starting 5min-post-injury. **(A)** Western blot (n=8/group) of hippocampal SBDP and total PARP at 24h-post-injury. **(B)** Western blot (n=8/group) of GFAP and IbA1 at 4d-post injury. **(C & D)** Densitometry of SBDPs and total PARP at 24h-post-injury (n=8/group). **(E & F)** Densitometry of GFAP and IbA1 at 4d-post-injury (n=8/group). Data were significant at $p < 0.05$. Asterisks in graphs indicate post hoc significance. (**) $p<0.01$, (***) $p<0.001$, (N.S.) = non-significant. Red highlighted p-value correspond to a N.S. trend on post-hoc.